ELSEVIER

Volume 230, October 2015

CONTENTS

JOURNAL OF SOLID STATE CHEMISTRY

www.elsevier.com/locate/jssc

Abstracted/indexed in BioEngineering Abstracts, Chemical Abstracts, Coal Abstracts, Current Contents/Physics, Chemical, & Earth Sciences, Engineering Index, Research Alert, SCISEARCH, Science Abstracts, and Science Citation Index. Also covered in the abstract and citation database SCOPUS®. Full text available on ScienceDirect®.

Regular Articles

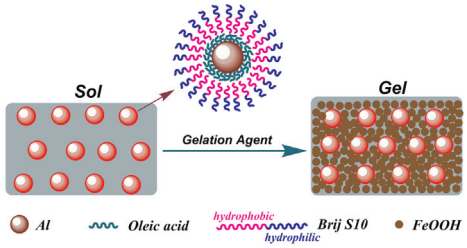

Modified aluminum (Al) nanoparticles with hydrophobic surface assembled into the Brij S10 micelle in Fe(III) sol, then the well dispersed system was transformed into Al/Fe_2O_3 nanoenergetic materials with high reactivity.

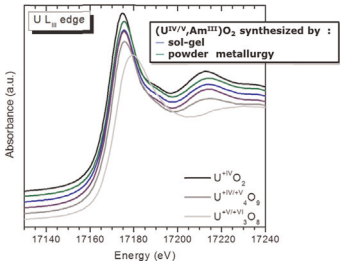

Formation of $(U^{IV/V},Am^{III})O^2$ solid solution by sol–gel and by powder metallurgy.

Regular Articles—Continued

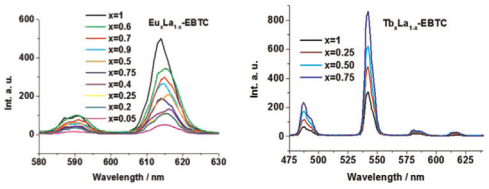

Two series of 3-D fluorescent lanthanide-MOFs-based molecular alloys RE_xLa_{1-x}–EBTC (RE^{3+}=Eu^{3+} or Tb^{3+}; $EBTC^{4-}$=1,1′-ethynebenzene-3,3′,5,5′-tetracarboxylate) have been successfully prepared by mixing Eu^{3+}/Tb^{3+} and La^{3+} salts with the desired molar ratio in the starting material and showed photoluminescence property with divergent La^{3+} ion dilute effect.

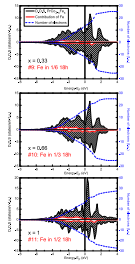

Total density of states (continuous black line, shaded area, left hand side scale), and number of electrons (dashed blue line, right hand side scale) of $PrCo_{3-x}Fe_x$ with spin polarization; (a) $x=\frac{1}{3}$, (b) $x=\frac{1}{6}$ and (c) $x=1$ with Fe occupying respectively $\frac{1}{6}$, $\frac{1}{3}$ and $\frac{1}{2}$ of 18*h* site. The white area limited by a red line corresponds to the only Fe contribution. The origin of the energy scale is located at the Fermi energy E_F.

Continued

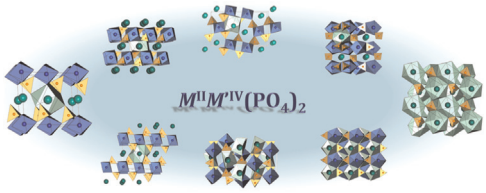

In this paper, the relationships between composition and crystal structure of $M^{II}M'^{IV}(PO_4)_2$ compounds are established. A review of the various processes used for the synthesis of these compounds is also proposed, as well as their most reported properties.

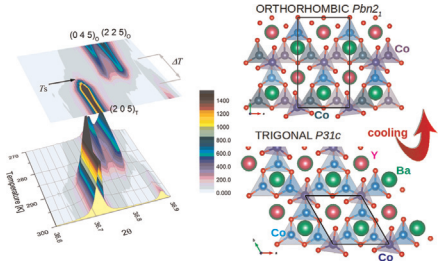

Thermal evolution of the diffractogram for a sample $YBaCo_{3.9}Ni_{0.1}O_{7.00}$ collected on cooling at the LNLS synchrotron source. The Bragg reflections were indexed in the trigonal $P31c$ and orthorhombic $Pbn2_1$ space groups above and below the transition temperature T_S, indicated with an arrow. The region of coexistence of both phases is indicated as ΔT. A projection along the c-axes for both crystal structures is shown on the right.

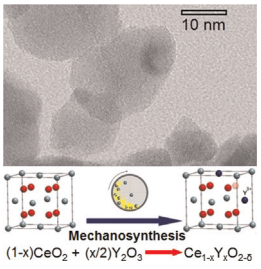

Mechanosynthesis of nanocrystalline $Ce_{1-x}Y_xO_{2-\delta}$ (x=0.1–0.35) solid solutions.

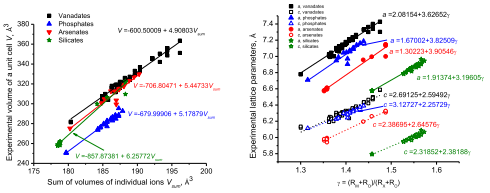

Correlation between the experimental volume of a unit cell and sum of volumes of individual ions (left) and correlation between the experimental lattice constants and $\gamma=(R_M+R_O)/(R_X+R_O)$ ratio in the group of 109 considered MXO_4 crystals (right).

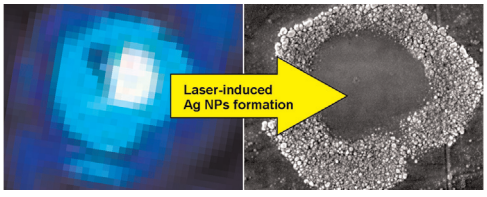

Formation of silver NPs on the surface of $0.5Ag_2O–0.4P_2O_5–0,1Nb_2O_5$ glass induced by CW laser irradiation.

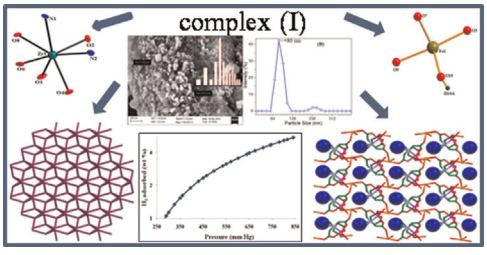

The complex (**I**) crystallized with unexpected coordination modes of EDTA having 4-c, 16-c net with new topology and point symbol is $(3^{36}.4^{54}.5^{30})\cdot(3^6)$. TGA study and XRPD pattern proved its stability with high preference of H_2 uptake by complex.